

Supplementary materials

An open chain carboxyethyltin functionalized sandwich-type tungstophosphate based on trivacant Dawson subunit: synthesis, characterization and properties

Jian-Ping Bai,^a Fang Su,^{a,b} Hao-Tian Zhu,^a Hang Sun,^a Lan-Cui Zhang,^{*a} Mei-Ying Liu,^a Wan-Sheng You^{*a} and Zai-Ming Zhu^{*a}

1. Crystal structure figures
2. Selected bond lengths and angles of SnR-Mn-P₂W₁₅
3. Physical characterizations
4. Catalysis experiments

1. Crystal structure figures

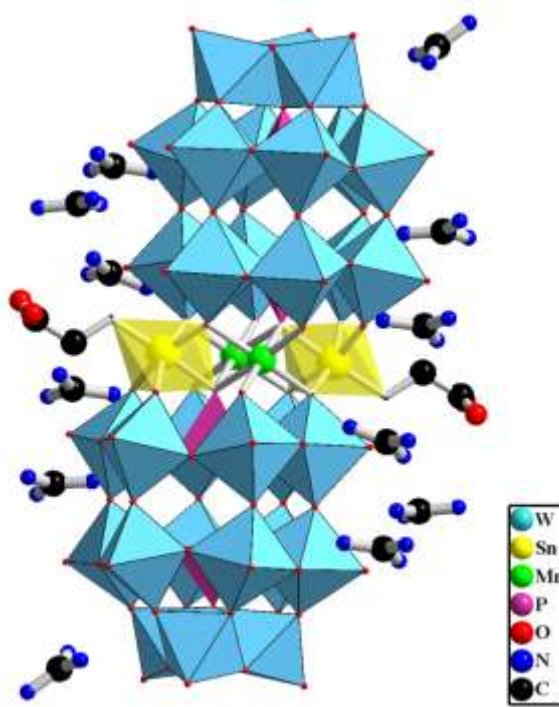


Fig. S1 Mixed ball-and-stick and polyhedral representation of **SnR-Mn-P₂W₁₅** (All hydrogen atoms and lattice water molecules are omitted for clarity)

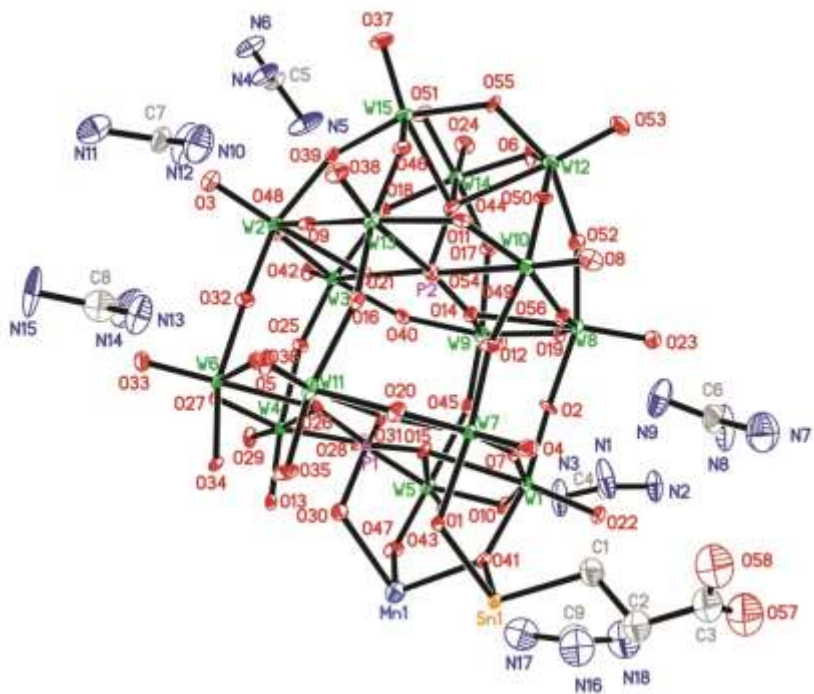


Fig. S2 ORTEP drawing of the polyoxoanion of **SnR-Mn-P₂W₁₅** with thermal ellipsoids at 30 % probability (Hydrogen atoms and free water molecules have been omitted for clarity)

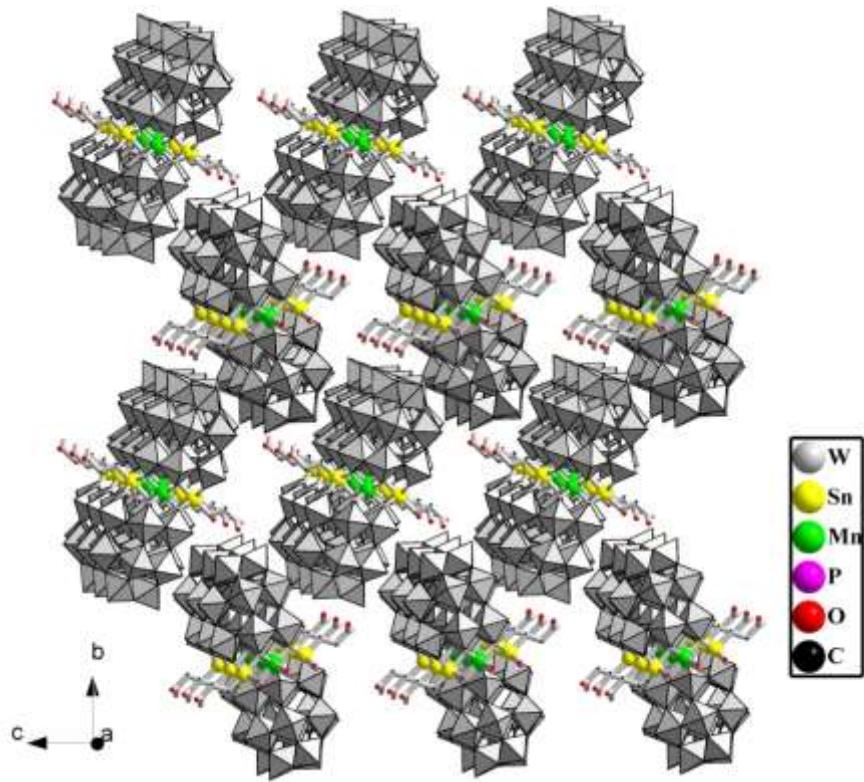
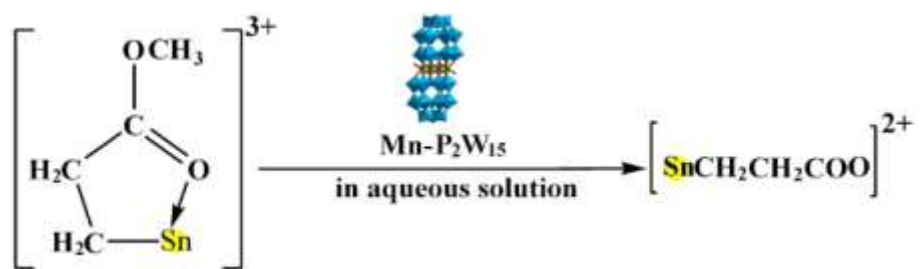


Fig. S3 The packing arrangement of the polyoxoanion in **SnR-Mn-P₂W₁₅** (All H atoms, the isolated [C(NH₂)₃]⁺ and water molecules existed in the interspaces are omitted for clarity)



Scheme S1 Hydrolysis of ester tin complex into open chain carboxyethyltin group during the synthetic process of **SnR-Mn-P₂W₁₅**

2. Selected bond lengths and angles of SnR-Mn-P₂W₁₅

Table S1 Selected bond lengths (Å) and angles (°) for SnR-Mn-P₂W₁₅

Bond	Length (Å)	Bond	Length (Å)	Bond	Length (Å)
W1–O22	1.702(11)	W7–O20	1.868(11)	W13–O46	2.034(11)
W1–O2	1.873(10)	W7–O7	1.906(10)	W13–O54	2.318(10)
W1–O10	1.884(10)	W7–O43	2.000(10)	W14–O24	1.725(11)
W1–O7	1.912(10)	W7–O31	2.389(10)	W14–O18	1.860(11)
W1–O41	2.010(10)	W8–O23	1.691(12)	W14–O17	1.868(11)
W1–O15	2.376(10)	W8–O8	1.885(10)	W14–O51	1.948(11)
W2–O3	1.695(12)	W8–O19	1.903(10)	W14–O6	1.975(12)
W2–O32	1.838(10)	W8–O56	1.904(10)	W14–O44	2.379(10)
W2–O9	1.881(10)	W8–O2	1.920(10)	W15–O37	1.715(12)
W2–O48	1.938(10)	W8–O14	2.388(11)	W15–O46	1.850(11)
W2–O39	1.995(11)	W9–O12	1.714(12)	W15–O39	1.873(11)
W2–O16	2.388(11)	W9–O45	1.799(10)	W15–O51	1.944(10)
W3–O42	1.703(10)	W9–O40	1.915(11)	W15–O55	1.972(11)
W3–O25	1.817(10)	W9–O19	1.941(10)	W15–O44	2.363(11)
W3–O40	1.872(11)	W9–O17	2.020(10)	Sn1–O34#1	2.069(11)
W3–O48	1.918(11)	W9–O14	2.337(10)	Sn1–O13#1	2.070(10)
W3–O18	1.993(10)	W10–O52	1.703(12)	Sn1–O41	2.098(10)
W3–O16	2.352(10)	W10–O50	1.875(10)	Sn1–O43	2.110(10)
W4–O29	1.720(11)	W10–O56	1.892(10)	Sn1–C1	2.16(2)
W4–O13	1.821(10)	W10–O11	1.896(11)	Sn1–O30#1	2.223(11)
W4–O28	1.909(11)	W10–O49	1.927(10)	Mn1–O47	2.043(11)
W4–O27	1.913(11)	W10–O54	2.382(10)	Mn1–O35#1	2.065(12)
W4–O25	2.005(10)	W11–O36	1.723(12)	Mn1–O43#1	2.129(11)
W4–O26	2.347(10)	W11–O35	1.776(12)	Mn1–O41	2.168(11)
W5–O1	1.745(11)	W11–O5	1.889(11)	Mn1–O30#1	2.291(11)
W5–O47	1.766(11)	W11–O20	1.982(11)	Mn1–O30	2.301(12)
W5–O28	1.911(11)	W11–O21	2.081(10)	P1–O31	1.530(10)
W5–O10	1.951(10)	W11–O31	2.334(10)	P1–O15	1.536(11)
W5–O45	2.106(10)	W12–O53	1.735(12)	P1–O26	1.540(12)

W5–O15	2.349(10)	W12–O55	1.875(11)	P1–O30	1.584(11)
W6–O33	1.713(12)	W12–O6	1.880(11)	P2–O16	1.523(11)
W6–O34	1.826(10)	W12–O8	1.941(11)	P2–O14	1.529(11)
W6–O5	1.914(11)	W12–O50	1.955(10)	P2–O54	1.534(10)
W6–O27	1.949(10)	W12–O44	2.412(11)	P2–O44	1.575(11)
W6–O32	1.987(10)	W13–O38	1.714(11)	C1–C2	1.514(10)
W6–O26	2.381(11)	W13–O21	1.790(10)	C2–C3	1.523(10)
W7–O4	1.718(11)	W13–O9	1.901(11)	C3–O57	1.279(10)
W7–O49	1.864(10)	W13–O11	1.958(12)	C3–O58	1.290(10)
Bond	Angle(°)	Bond	Angle(°)	Bond	Angle(°)
O22–W1–O15	172.6(4)	O49–W7–O43	166.0(4)	O11–W13–O54	73.5(4)
O2–W1–O41	167.4(5)	O20–W7–O31	73.2(4)	O46–W13–O54	79.4(4)
O10–W1–O15	72.4(4)	O43–W7–O31	80.5(4)	O24–W14–O44	168.1(5)
O7–W1–O41	84.7(4)	O23–W8–O14	172.2(5)	O18–W14–O6	157.0(5)
O3–W2–O16	172.0(5)	O8–W8–O2	160.0(5)	O51–W14–O44	71.2(4)
O32–W2–O39	162.3(5)	O19–W8–O14	73.0(4)	O6–W14–O44	72.8(4)
O48–W2–O16	72.9(4)	O2–W8–O14	78.2(4)	O37–W15–O44	167.9(5)
O39–W2–O16	79.6(4)	O12–W9–O14	170.0(5)	O39–W15–O55	158.4(4)
O42–W3–O16	171.6(5)	O45–W9–O17	162.6(4)	O51–W15–O44	71.6(4)
O25–W3–O18	161.5(4)	O19–W9–O14	73.6(4)	O55–W15–O44	72.7(4)
O48–W3–O16	74.1(4)	O17–W9–O14	79.3(4)	O34#1–Sn1–O41	88.7(4)
O18–W3–O16	79.0(4)	O52–W10–O54	171.0(5)	O13#1–Sn1–O43	89.5(4)
O29–W4–O26	174.2(5)	O50–W10–O49	161.6(5)	C1–Sn1–O30#1	176.6(6)
O13–W4–O25	164.0(4)	O11–W10–O54	73.0(4)	O41–Sn1–C1	103.0(7)
O27–W4–O26	74.2(4)	O49–W10–O54	78.7(4)	O35#1–Mn1–O30	176.6(4)
O25–W4–O26	82.5(4)	O36–W11–O31	170.5(4)	O47–Mn1–O30#1	175.2(5)
O1–W5–O15	169.5(5)	O35–W11–O21	165.7(5)	O43#1–Mn1–O30	77.3(4)
O47–W5–O45	166.6(4)	O20–W11–O31	72.6(4)	O41–Mn1–O30#1	76.7(4)
O10–W5–O15	72.0(4)	O21–W11–O31	81.0(4)	O31–P1–O15	111.9(6)
O10–W5–O45	82.0(4)	O53–W12–O44	174.1(5)	O31–P1–O26	111.2(6)
O33–W6–O26	173.3(5)	O6–W12–O50	155.9(5)	O15–P1–O30	108.0(6)
O34–W6–O32	163.1(5)	O55–W12–O44	73.1(4)	O16–P2–O14	111.8(6)
O34–W6–O26	81.0(4)	O6–W12–O44	73.5(4)	O14–P2–O54	112.8(6)

O27–W6–O26	72.8(4)	O38–W13–O54	170.7(5)	O14–P2–O44	106.7(6)
O4–W7–O31	170.5(5)	O21–W13–O46	162.4(4)		

Symmetry transformations used to generate equivalent atoms: #1 -x+1,-y,-z

Table S2 Hydrogen bonds for **SnR-Mn-P₂W₁₅**

D–H···A	d(D–H) (Å)	d(H···A) (Å)	d(D···A) (Å)	∠(DHA) (°)
N1–H1C···O10	0.86	2.08	2.916(18)	163.3
N1–H1D···O37#2	0.86	2.04	2.90(2)	177.0
N2–H2C···O4#3	0.86	2.21	3.044(19)	163.4
N2–H2D···O51#2	0.86	2.17	3.01(2)	164.1
N3–H3A···O20#3	0.86	2.05	2.89(2)	164.0
N3–H3B···O1	0.86	2.16	3.01(2)	170.0
N4–H4A···O39	0.86	2.14	2.995(18)	170.5
N4–H4B···O19#4	0.86	1.99	2.840(18)	172.2
N5–H5A···O18	0.86	2.13	2.90(2)	149.5
N5–H5A···O48	0.86	2.62	3.26(2)	132.9
N5–H5B···O52#5	0.86	2.13	2.96(2)	161.3
N6–H6A···O12#4	0.86	2.03	2.89(2)	174.2
N6–H6B···O11#5	0.86	2.10	2.93(2)	163.5
N7–H7A···O23	0.86	2.38	3.12(3)	144.5
N7–H7A···O37#2	0.86	2.63	3.12(2)	116.9
N7–H7B···O3W#2	0.86	2.48	3.24(4)	148.0
N7–H7B···O46#2	0.86	2.54	3.18(2)	131.7
N8–H8A···O24#6	0.86	2.46	3.18(3)	142.0
N8–H8B···O3W#2	0.86	2.59	3.34(4)	145.4
N9–H9A···O24#6	0.86	2.20	3.00(2)	154.1
N9–H9B···O56	0.86	2.36	3.13(2)	147.7
N10–H10A···O38	0.86	2.54	3.27(2)	142.8
N10–H10A···O9	0.86	2.60	3.30(2)	140.4
N11–H11A···O53#4	0.86	2.32	3.17(2)	172.2
N11–H11B···O42#7	0.86	2.16	3.00(2)	165.0
N12–H12A···O38	0.86	2.25	3.05(2)	155.3
N13–H13A···O28#7	0.86	2.26	3.088(19)	160.3
N13–H13B···O36	0.86	2.13	2.92(2)	152.2
N14–H14A···O36	0.86	2.41	3.13(2)	140.8
N14–H14A···O5	0.86	2.63	3.37(2)	145.3
N14–H14B···O4W	0.86	2.18	2.99(5)	157.7
N15–H15A···O29#7	0.86	2.18	2.98(2)	155.7
N15–H15B···O4W	0.86	2.50	3.24(5)	144.7
N16–H16B···O35#1	0.86	2.26	3.03(3)	149.5
N16–H16B···O34#1	0.86	2.55	3.16(2)	128.7
N17–H17A···O35#1	0.86	2.23	3.00(2)	149.3
N17–H17B···O1#8	0.86	2.34	2.99(2)	131.8
N18–H18B···O2W#3	0.86	1.97	2.82(3)	170.9

Symmetry transformations used to generate equivalent atoms: #1 -x+1,-y,-z; #2 x+1/2,-y+1/2,z+1/2; #3 x+1,y,z;

#4 x-1/2,-y+1/2,z-1/2; #5 x+1/2,-y+1/2,z-1/2; #6 x-1/2,-y+1/2,z+1/2; #7 x-1,y,z; #8 -x+2,-y,-z

3. Physical characterizations

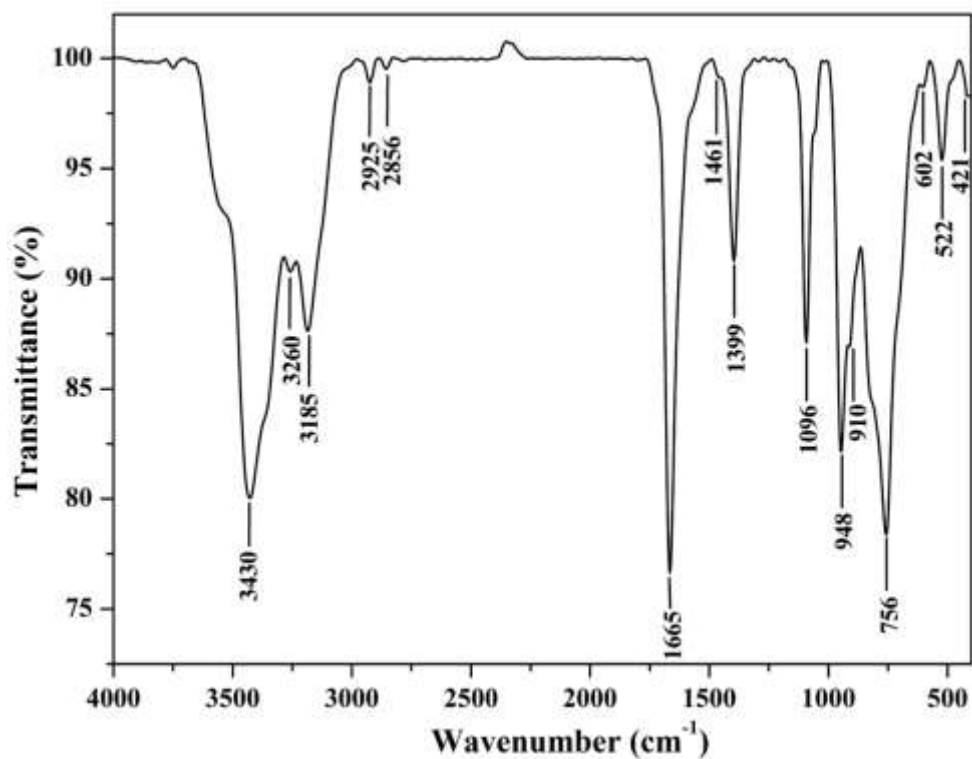


Fig. S4 The IR spectrum of SnR-Mn-P₂W₁₅

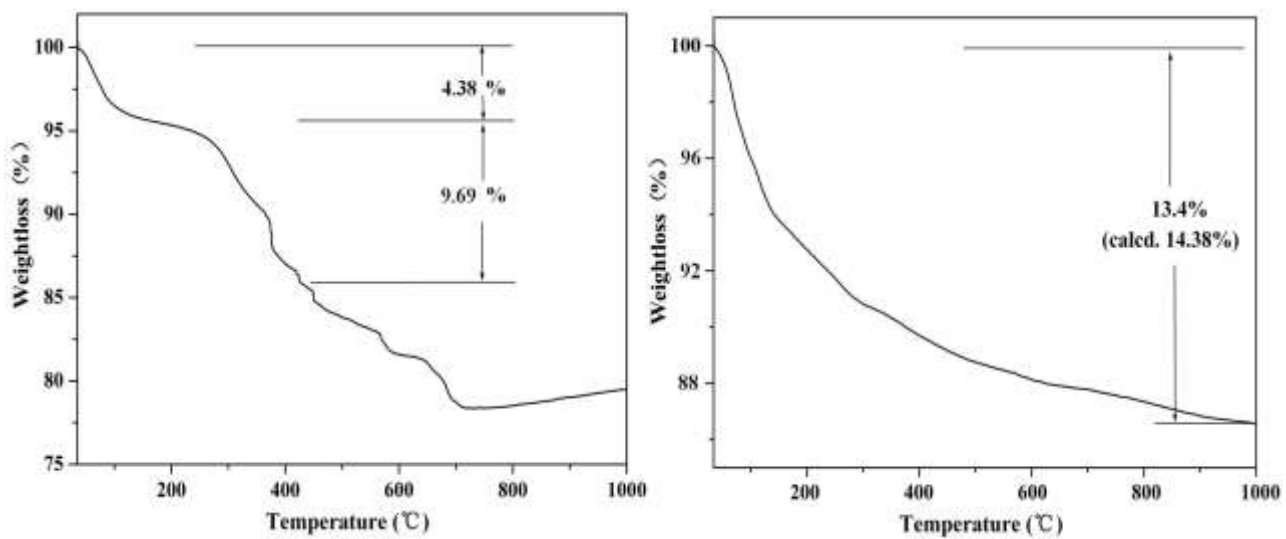


Fig. S5 TG curves of SnR-Mn-P₂W₁₅ (a) and Mn-P₂W₁₅ (b)

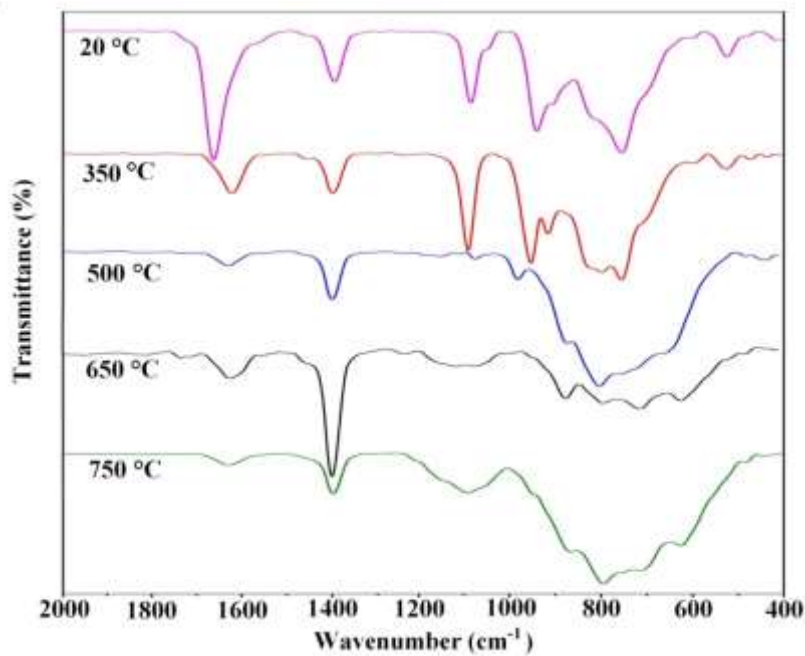


Fig. S6 The IR spectra of **SnR-Mn-P₂W₁₅** at different temperatures. At 350 °C, the characteristic peaks of polyanion at 1096, 948, 910, 756 cm⁻¹ (20 °C) belonging to $\nu(\text{P}-\text{O})$, $\nu(\text{W}=\text{O}_d)$, $\nu(\text{W}-\text{O}_a)$, $\nu(\text{W}-\text{O}_b)$ and $\nu(\text{W}-\text{O}_c)$ respectively still retain, indicating the existence of intrinsic sandwich-type structure. After 500 °C, the $\nu_{as}(\text{COO}^-)$ and $\nu_s(\text{COO}^-)$ vibrations at 1618 and 1358 cm⁻¹ disappeared, which illustrated the decomposition of organatin groups. Furthermore, the peak of P–O vibration become weaker, meaning that the polyoxoanion skeleton collapsed, and resulting in the obvious weight loss in the TG curve

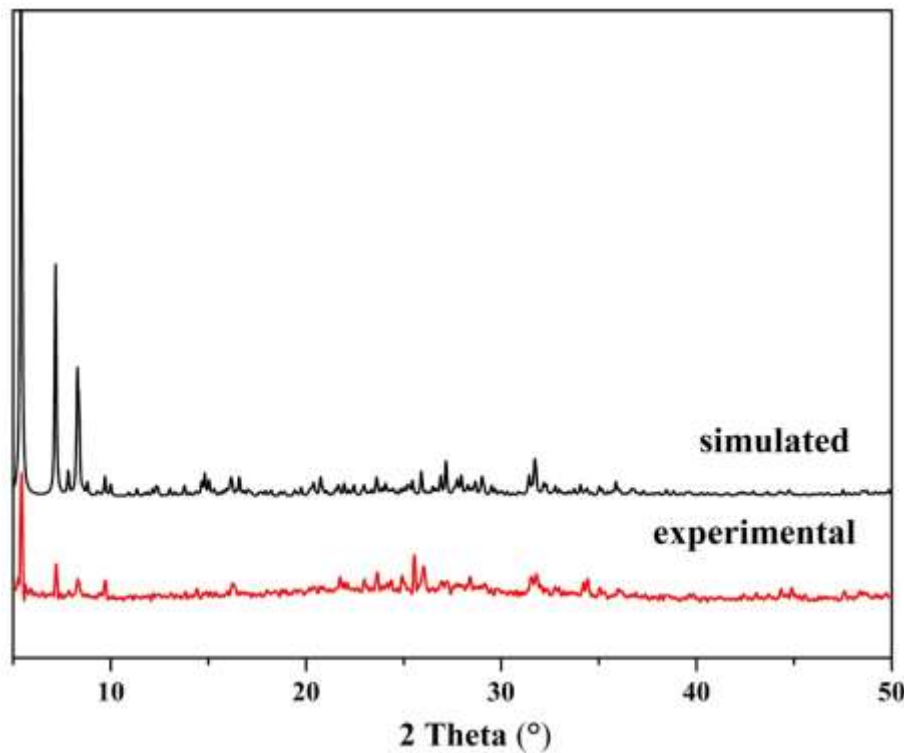


Fig. S7 The simulated and experimental XRPD patterns of **SnR-Mn-P₂W₁₅**

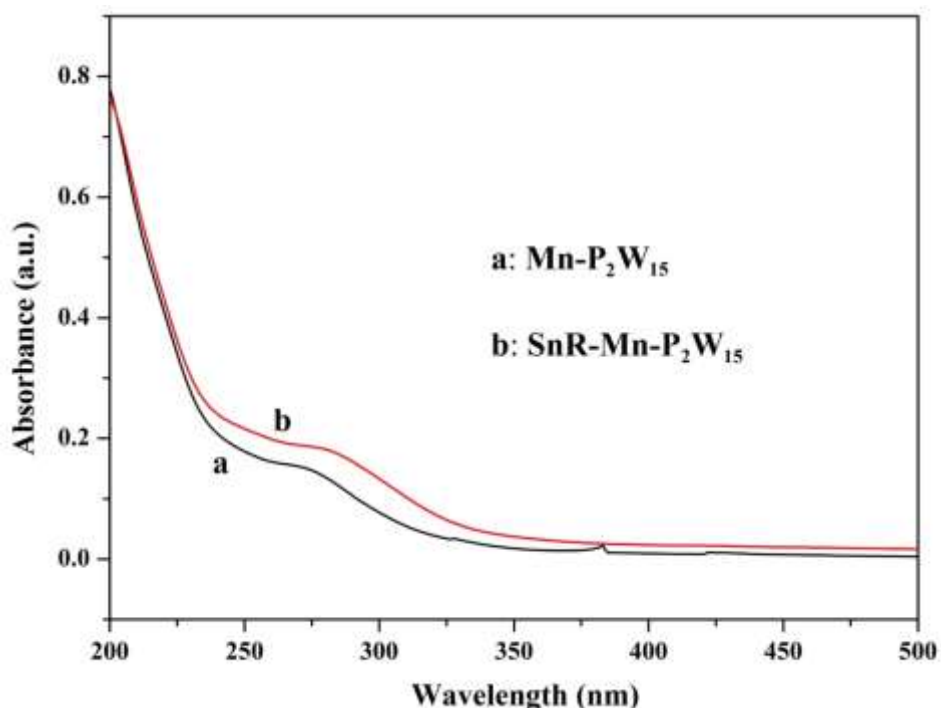


Fig. S8 UV-vis absorption spectra of $\text{SnR-Mn-P}_2\text{W}_{15}$ and $\text{Mn-P}_2\text{W}_{15}$ in NaCl aqueous solution, respectively

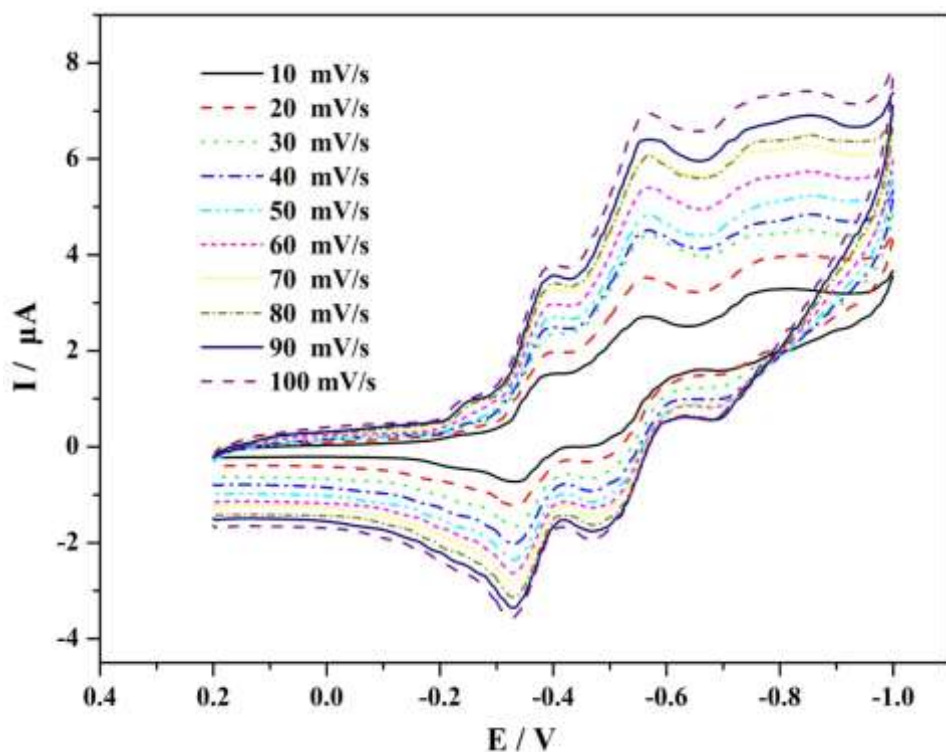


Fig. S9 Cyclic voltammogram of $\text{SnR-Mn-P}_2\text{W}_{15}$ in $1 \text{ mol L}^{-1} \text{Na}_2\text{SO}_4\text{-H}_2\text{SO}_4$ aqueous solution ($\text{pH} = 4$) at different scan rates

4. Catalysis experiments

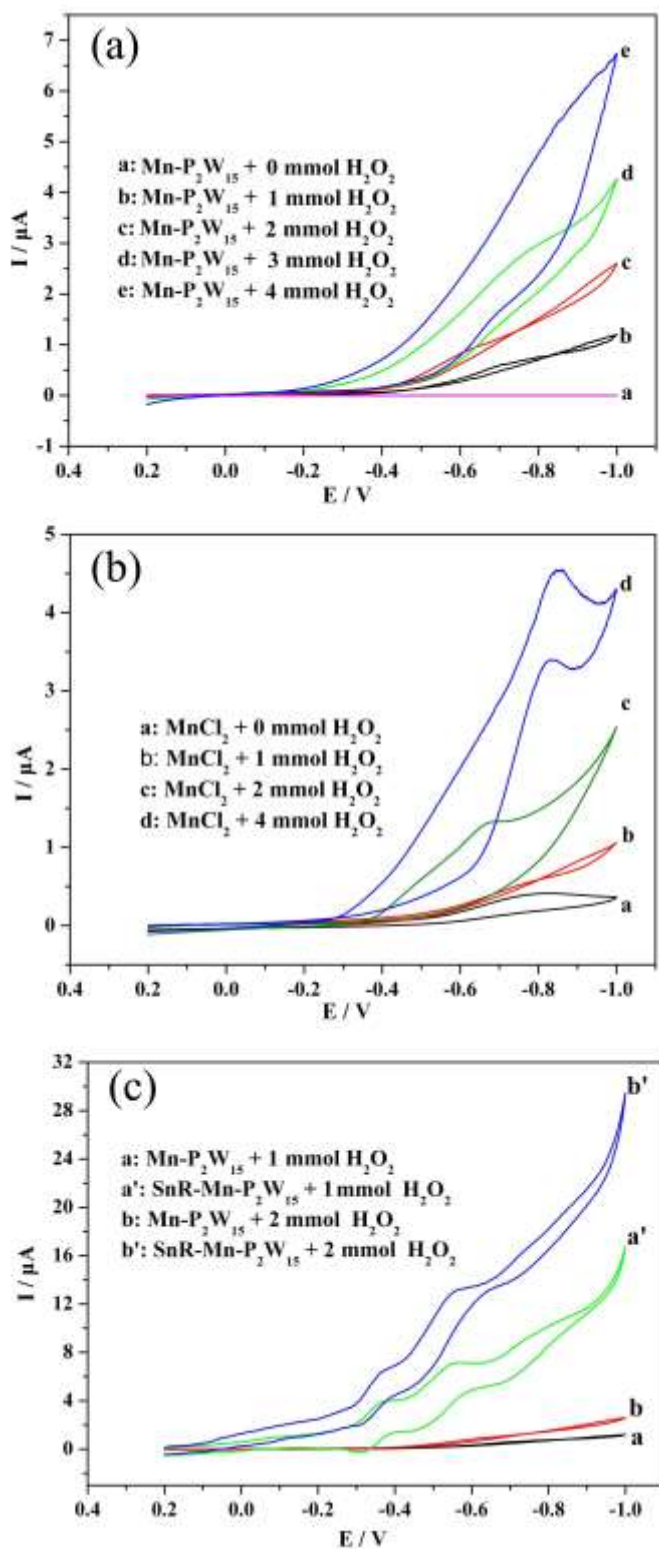


Fig S10 Electrocatalytic reduction of H_2O_2 with a $1.0 \times 10^{-4} \text{ mol L}^{-1}$ solution of $\text{Mn-P}_2\text{W}_{15}/\text{MnCl}_2$ in a 1 mol L^{-1} $\text{Na}_2\text{SO}_4-\text{H}_2\text{SO}_4$ aqueous solution (pH = 4) at the scan rate of 50 mV s^{-1} . (a) $\text{Mn-P}_2\text{W}_{15}$; (b) MnCl_2 ; (c) Comparison of $\text{SnR-Mn-P}_2\text{W}_{15}$ and $\text{Mn-P}_2\text{W}_{15}$

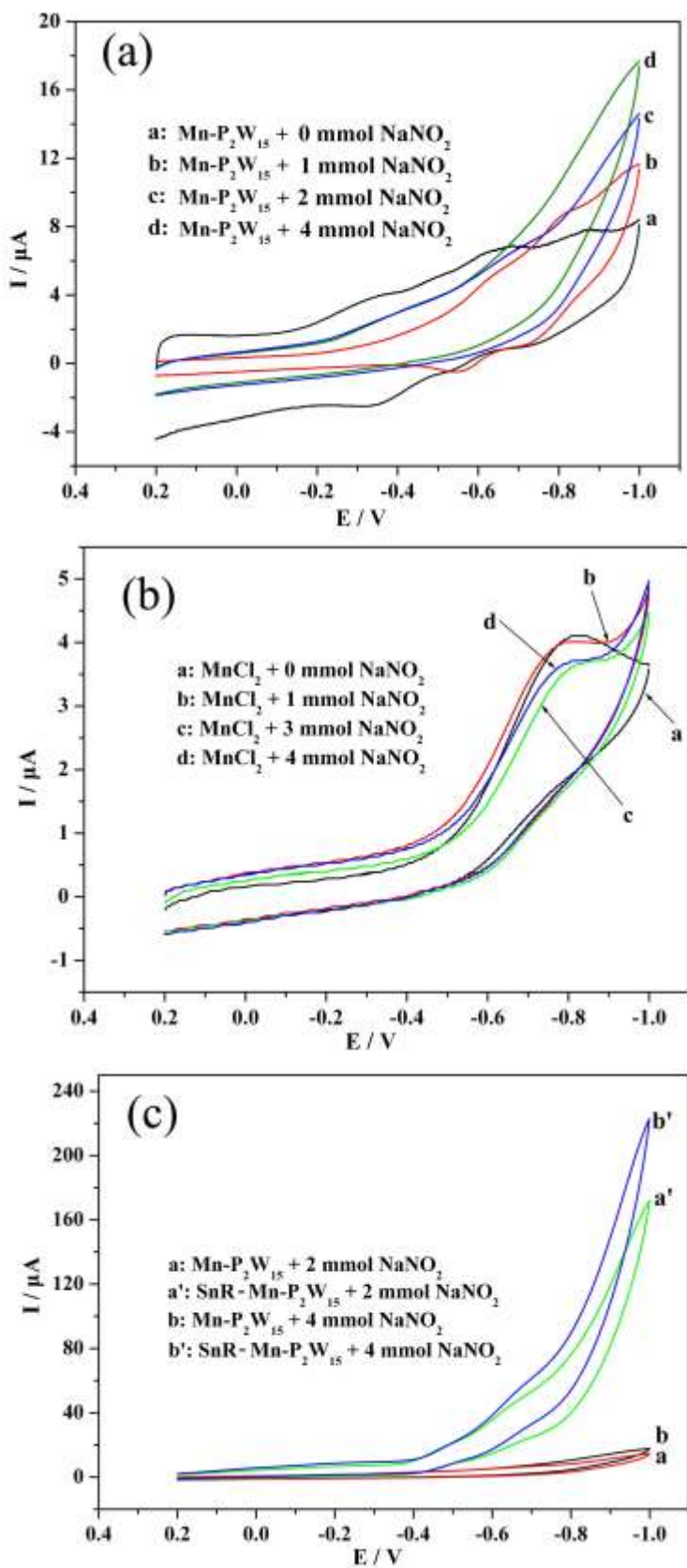
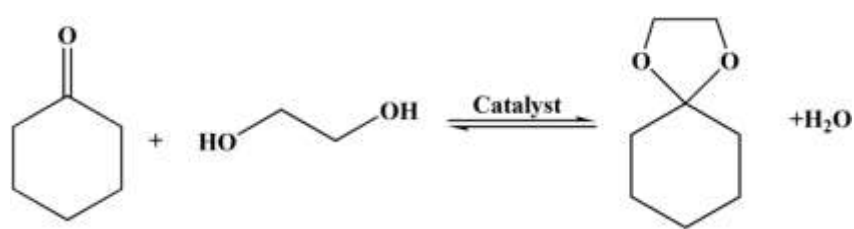


Fig S11 Electrocatalytic reduction of NaNO_2 with a $1.0 \times 10^{-4} \text{ mol L}^{-1}$ solution of $\text{Mn-P}_2\text{W}_{15}/\text{MnCl}_2$ in a 1 mol L^{-1} $\text{Na}_2\text{SO}_4\text{-H}_2\text{SO}_4$ aqueous solution ($\text{pH} = 4$) at the scan rate of 50 mV s^{-1} . (a) $\text{Mn-P}_2\text{W}_{15}$; (b) MnCl_2 ; (c) Comparison of $\text{SnR-Mn-P}_2\text{W}_{15}$ and $\text{Mn-P}_2\text{W}_{15}$.



Scheme S2 Ketalization of cyclohexanone with glycol

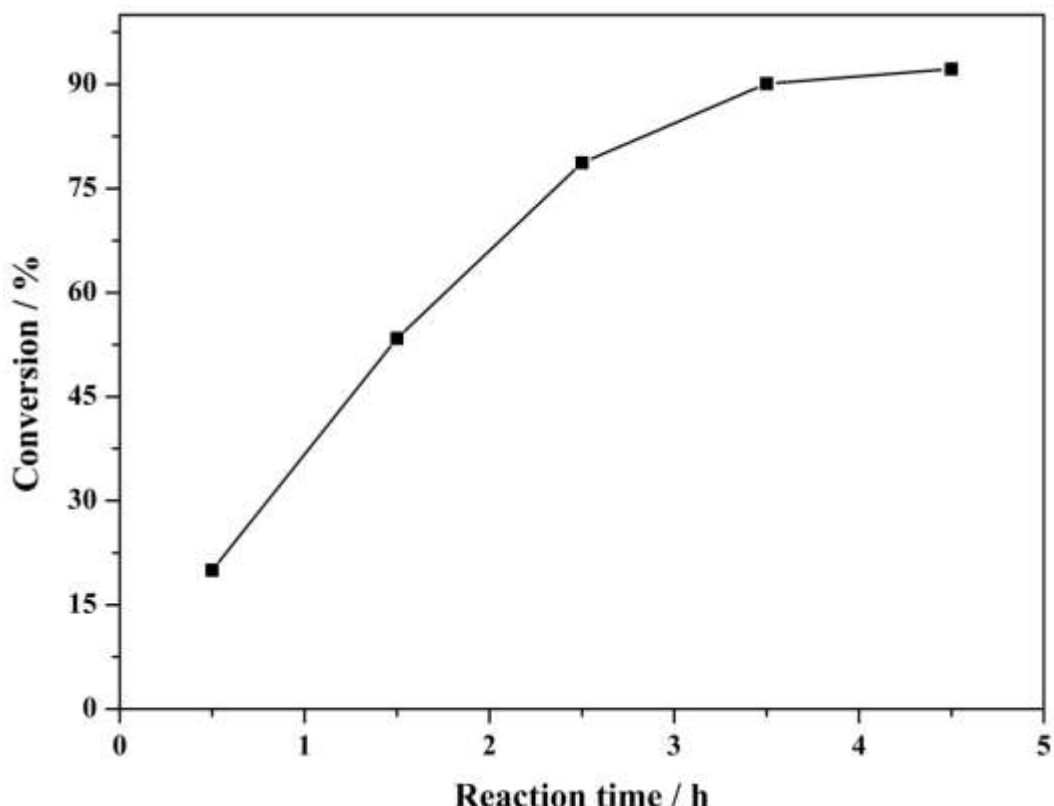


Fig. S12 Influence of reaction time on cyclohexanone ethylene ketal productivity: cyclohexanone (0.1 mol)/glycol molar ratio, 1:1.4; **SnR-Mn-P₂W₁₅** (based on W)/cyclohexanone molar ratio, 1:200; reaction temperature, 95–100 °C; water-carrying agent, cyclohexane (10 mL)

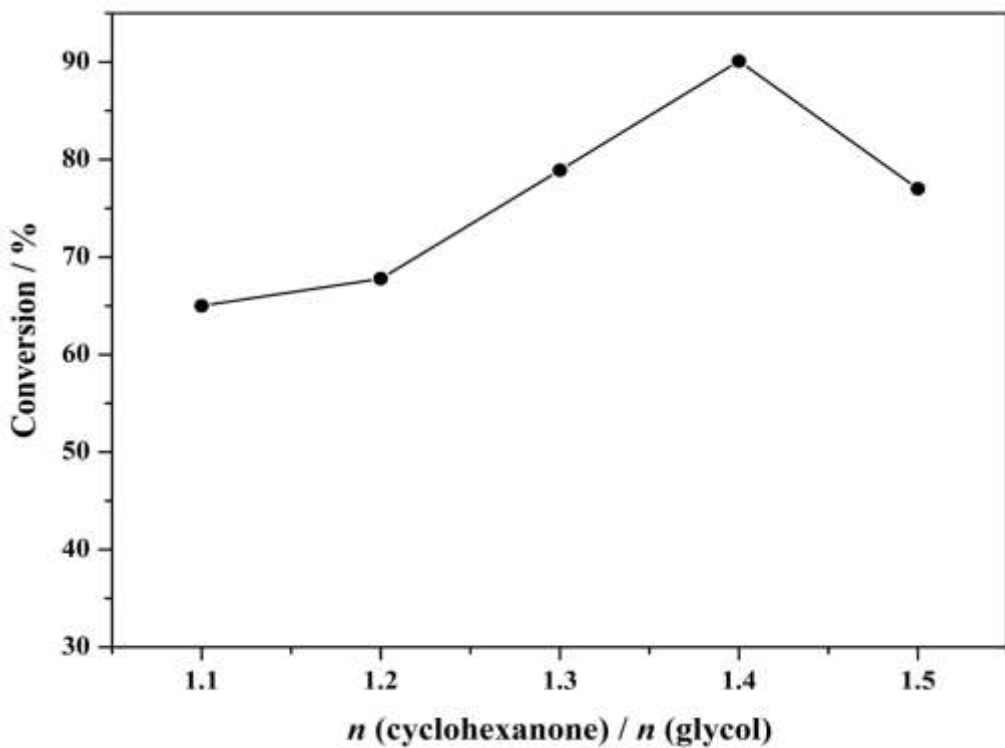


Fig. S13 Influence of the material ratio on cyclohexanone ethylene ketal productivity: **SnR-Mn-P₂W₁₅** (based on W)/cyclohexanone (0.1 mol) molar ratio, 1:200; reaction temperature, 95-100 °C; reaction time, 3.5 h. water-carrying agent, cyclohexane (10 mL)

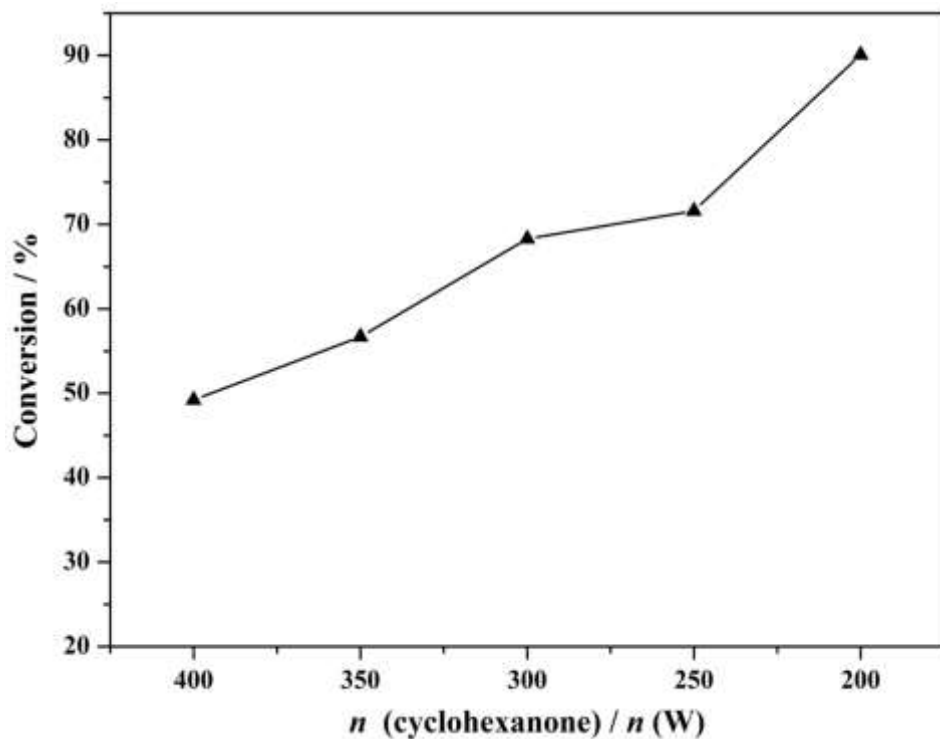


Fig. S14 Influence of the amount of **SnR-Mn-P₂W₁₅** on cyclohexanone ethylene ketal productivity: cyclohexanone (0.1 mol)/glycol molar ratio, 1:1.4; reaction temperature, 95-100 °C; reaction time, 3.5 h; water-carrying agent, cyclohexane (10 mL)

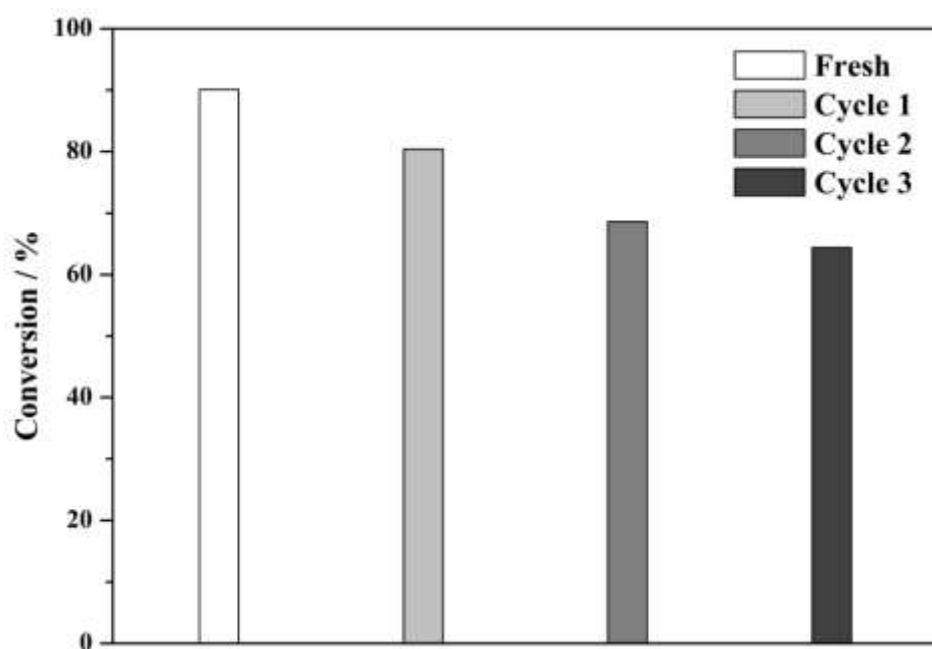


Fig. S15 The catalytic activities of **SnR-Mn-P₂W₁₅** used four cycles for the synthesis of cyclohexanone ethylene ketal, and catalyst was recovered by simple filtration without any treatment. The reaction conditions: catalyst (based on W)/cyclohexanone (0.1 mol) molar ratio, 1:200; cyclohexanone (0.1 mol)/glycol molar ratio, 1:1.4; reaction temperature, 95–100 °C; reaction time, 3.5 h; water-carring agent, cyclohexane (10 mL)

Table S3 Catalytic performance of catalysts **SnR-Mn-P₂W₁₅**, the parent **Mn-P₂W₁₅**, monomer **P₂W₁₅**, **Cl₃SnCH₂CH₂COOCH₃** and **MnCl₂** for the synthesis of cyclohexanone ethylene ketal

Entry	Catalyst	Solubility	Time (h)	Yield (%)
1	P₂W₁₅	insoluble	3.5	6
2	Mn-P₂W₁₅	insoluble	3.5	10
3	Cl₃SnCH₂CH₂COOCH₃	soluble	3.5	97
4	MnCl₂	soluble	3.5	86
5	SnR-Mn-P₂W₁₅	insoluble	3.5	90

Table S4 Catalytic performance of various catalysts for the oxidation of cyclohexanol to cyclohexanone with H₂O₂

Entry	Catalyst	H ₂ O ₂ (equiv.)	Solvent	Solubility	Temperature (°C)	Time (min)	Isolated yield (%)
1	P₂W₁₅	2.2	MeCN	soluble	80	150	70.9
2	Mn-P₂W₁₅	2.2	MeCN	soluble	80	150	16.7
3	MnCl ₂	2.2	MeCN	soluble	80	150	7.7
4	Cl ₃ Sn(CH ₂) ₂ COOCH ₃	2.2	MeCN	soluble	80	150	34.5
5	SnR-Mn-P₂W₁₅	2.2	MeCN	soluble	80	150	72.4